

# THE POTENTIAL CARBON LOSSES ESTIMATION WITH REMOTE SENSING-BASED DATA: CASE STUDY IN NOVA VIDA RANCH, RONDONIA, BRAZIL

Lyu Lingbing, SHEN Jing

QICS, No.28 Lianhuachi West Road, Haidian District, Beijing, 100830 – lvlinbing0728@163.com

**KEY WORDS:** Carbon potentials, Carbon losses, Land cover changes, Deforestation.

## ABSTRACT:

Carbon losses have enormous impacts on ecosystem and indicative meaning for ecological stability, which are, therefore, necessary to be evaluated. In recent years, with the increasingly number of people settling in Amazon basin, large areas of tropical forests have been exploited, which took the mainly responsible for local deforestation.

Carbon losses are hardly to be evaluated directly but can be inferred from the relationship between potential carbon and forest structures referring to previous studies. Remote sensing-based methods are widely used because of the obvious advantages of, such as the repeatability of data collection, high correlations between spectral bands and vegetation parameters etc. However, the selection of the spatial resolution of data is a critical issue that should be taken into consideration for it influences the performance of image texture thereby the discrimination of land covers, especial in complex forest stand structure. The approach for image feature extraction used in the study is explained.

Based on the available datasets, this study aims to estimate the potential carbon losses across selected plot in Nova Vida Ranch, Rondônia, Brazil between 1989 and 2001. The results showed that carbon potentials decreased at least  $1.1 \times 10^8$  (Kg C) during the 12 years, which would affect all the climate, wildlife habitats and biodiversity. The study suggested that it is significantly important to reduce the uncertainties that are caused by saturation in some of the tropic areas. To pursue this, the research on the integration of optical and radar data is worth to experiment in further study.

## 1. INTRODUCTION

In recent years, with the increasingly number of people settling in Amazon basin, large areas of tropical forests have been exploited. whatever the various purposes of exploitation were, for example, timber extraction, shifting cultivation, permanent agriculture and pasture (Moraes et al, 1998), at least 50% of tropical forest areas, were converted to agricultural lands from 1980s to 1990s, which took the mainly responsible for local deforestation (Myers, 1991).

Carbon loss due to deforestation and degradation has enormous impacts on ecosystem (Myers, 1991), and thus it is important to monitor the losses. Carbon losses are hardly to be evaluated directly but can be inferred from the relationship between potential carbon and forest structures referring to previous studies (Lu, 2006, Moraes et al, 1998, Steininger, 2000, Foody et al, 2003, Zheng et al, 2004). Many cases showed that traditional field measurements, remote sensing and GIS, were mainly used for estimation (Lu, 2006). Among them, remote sensing-based methods are widely used (Moraes et al, 1998, Steininger, 2000, Foody et al, 2003, Zheng et al, 2004), depending on the advantages of remote sensed data on estimating biomass (Lu, 2006), such as the repetititvity of data collection, high correlations between spectral bands and vegetation parameters etc.. For example, Liu et al (2020) calculated carbon loss through the changes of land use and land cover changes (LULCC) in wetland. Zheng et al (2004) bridges the application of remote sensing techniques with various forest management practices in Chequamegon National Forest, Wisconsin, USA by producing a high-resolution stand age map and a spatially explicit above-ground biomass (AGB) map. Lu (2006) chose Landsat Thematic Mapper (TM) data to estimate AGB in relatively simple forest structure areas.

Based on the available datasets, this paper aims to estimate the potential losses across the selected plot in Nova Vida Ranch,

Rondônia, Brazil between 1989 and 2001. Firstly, deforestation is detected by analysing the LULCCs. In order to improve the discrimination of land covers (LCs), especial in complex forest stand structure, principal component analysis (PCA) is adopted in the study to enhance the ability of extraction of image features. Secondly, based on the carbon potentials for different types of land covers, the losses of carbon potentials are estimated, and the causes of loss are also discussed.

## 2. METHOD

### 2.1 Study area

The study area (covering about  $375 \text{ km}^2$ ) is located in the southwestern Brazilian Amazon basin, in Rondonia state (Figure 1). The experimental site is conducted at Nova Vida Ranch (NVR) where has total area of 22000 ha ( $220 \text{ km}^2$ ) (Graca et al, 1999). The climate of NVR is humid tropical with high annual precipitation of 2200mm (Bastos and Diniz, 1982).

Natural vegetation has been classified as ‘open humid tropical forest’ and mainly consist of palm trees (Pirez and Prance, 1985). Two main soil types are classified by Moraes et al (1998) in terms of U. S. soil taxonomy, including Kandiudult (red yellow podzolic latosolic) and Ultisol (red yellow podolic soil). Both of them cover almost 60 per cent of the area of Amazon basin.

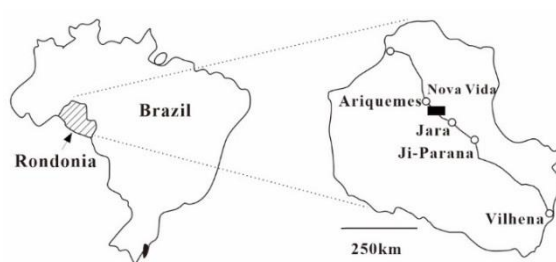


**Figure 1** Study area. Modified from: Moraes et al, 1998

## 2.2 Carbon losses estimation

The calculation of the carbon losses between 1989 and 2001 requires the knowledge of the areas of LULCC during this time period and the AGB estimate in different LC features. Olson et al (1983) summarised carbon potentials in major world ecosystem complexes, which provided the relevant carbon stored data. In that case, the LULCC is detected using post classification method.

### 2.2.1 Data pre-processing

Geometric correction is required in data pre-processing by using image to image registration that is used to geometrically aligns two images taken at different times and / or by different sensors (Zitova and Flusser, 2003). The two Landsat data that the early one (1989) is from Thematic Mapper (TM) sensor and the later one (2001) is from Enhanced Thematic Mapper (ETM). Ten ground control points (GCPs) are chosen and the RMS was controlled within 0.1103 to get more accurate registration, as poor geometric accuracies could result in false relationships between AGB and the remote sensed data (Halme and Tomppo, 2001).

### 2.2.2 Land cover (LC) classification

LC classification is conducted using supervised classification method. According to the previous studies on LC types in Nova Vida Ranch and Amazon basin (Moraes et al, 1998, Braswell et al, 2003), the LC are classified into 4 broad types including forest, soil/sparse grass (SSG), grassland and non-vegetation features (NVF). The details are showed in Table 1.

Broad Types	Content	Colour
Forest	Woodland Dense vegetation	Green
Soil /Sparse grass (SSG)	Bare soil Sparse grass	Sienna
Grassland	Pasture Agricultural land	Yellow
Non-vegetation features (NVF)	Urban area (Major type) Road Unknown	Magenta

**Table 1** Land cover classification.

Training samples are collected for supervised classification, of which the collected pixel should be as few, according to Moraes et al (1998) suggested of range of three to six, and homogenous(uniformly coloured area) as possible, because the high number of pixels results in high standard deviation thereby decreasing the classification accuracy (Moraes et al, 1998, Gong and Howarth, 1992). To ensure all types of textures within same LCs can be collected, it is no doubt to increase the workloads.

A combination of spectral responses and image textures improves biomass estimation performance (Lu, 2006), since spectral information can help compensating textural losses in some degree. Principal component analysis (PCA) is adopted in this study and spectral signature is also used to detect the same LC types. Since PCA can convert a set of relevant variables into another group of irrelevant variables by linear transformation (Lin et al, 2012, Zhao et al, 2012) and can also reduce the

topographic effects on vegetation reflectance. According to Li et al (2014), the first principal component (PC-1) is required to have the largest possible variance and the result of PCA show that the PC-1 obtain the highest eigenvalues in both images (Figure 2). Therefore, the PC-1 images are used to compare with true colour images to identify the LC types. Based on the characteristics of remotely sensed data, same LC features have similar spectral signals, which is conducive to classify the features that are too fragmented to identify from the images. Finally, both images are classified based on the training samples that are collected by using region of interest (ROI) function in ENVI.

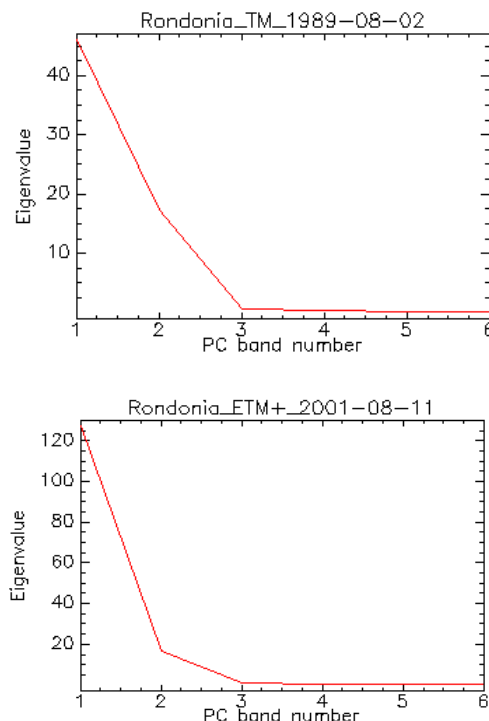


**Figure 2** The result of principal component analysis; left: TM; right : ETM

### 2.2.3 Carbon losses estimation

The carbon potentials provided by Olson et al (1983) are estimated in world ecosystem scale thereby not very precisely. Therefore, instead of exact data, median and estimated range are adopted. Olson demonstrated the carbon potentials in specific types of LCs and corresponding to the environments of this study area, the following categories and values are considered reasonably to be adopted, as showed in Table 2.

The carbon balances are estimated based on the LULCCs and the carbon potentials for each type of LC. The equation (Eq. 1) is showed as follow.

*Carbon balance =*

$$\sum \text{carbon potentials}_i \times \text{Area}_{Ii} - \sum \text{Carbon potential}_i \times \text{Area}_{Fi} \quad (1)$$

where *i* is the type of LC, *Ii* is the initial area of each LC in 1989 and *Fi* is the final area in 2001.

### 3. ULTS AND DISCUSSION

#### 3.1 Land cover changes

In 1989, the LC types consisted mainly of forest and SSG. The distributions of grasslands were scattered around the margin of the forest and that of NVFs were relative concentrated. While in 2001, the primary LC types were forest, grassland and NVFs. The original SSG lands were almost disappeared (Figure 3). As can be seen from Figure 4, the proportion of SSG decreased from 21 per cent to 7 per cent and that of forest also shrank from 55 per cent to 48 per cent. In the contrast, the proportions of grassland and NVFs grew 12 and 9 per cent respectively.

Land cover	Category	Carbon potentials Median (Kg C/m <sup>2</sup> )	Carbon potentials Range (Kg C/m <sup>2</sup> )
Forest	Main tropical forest (broad-leaved humid forest)	12	4 -25
Grassland	Grass and shrub complexes (main grassland, warm and hot)	0.9	0.5-3
Soil / Sparse grass (SSG)	Heath	1.0	1-2
Non-vegetation features (NVF)	Marginal Lands (warm or hot settlements)	0.8	0.6-2

**Table 2** Carbon potentials estimated for land covers

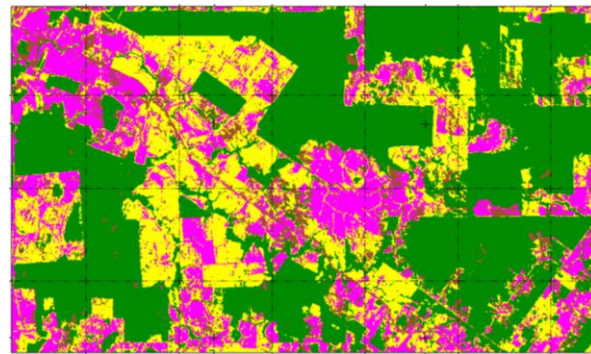
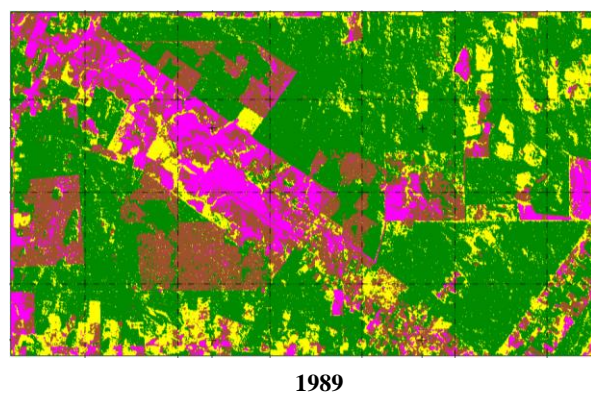


**Figure 3** The results of land cover classifications in 1989 (a) and 2001 (b). Forest (green); Soil / Sparse grass (sienna), Grassland (yellow), Non-vegetation features (magenta).

The specific changing patterns are showed in Figure 4 a, b, c, d and statistic results are showed in Table 3. Firstly, forest areas were mainly replaced by NVFs and grassland. The total deforestation area was 24.75 km<sup>2</sup>. Secondly, it is notable that almost all the original SSG lands were almost replaced by grassland and NVFs. The total SSG loss was 49.92 km<sup>2</sup>. Thirdly, Urban areas (NVFs) increased significantly across the experimental area during the period of time, however, parts of original areas were replaced by grassland. The total expansion was 32.32 km<sup>2</sup>. Finally, grassland area also had a dramatic increase, while only a small part of original grassland was replaced. From 1989 to 2001, grassland area grew 42.34 km<sup>2</sup>.

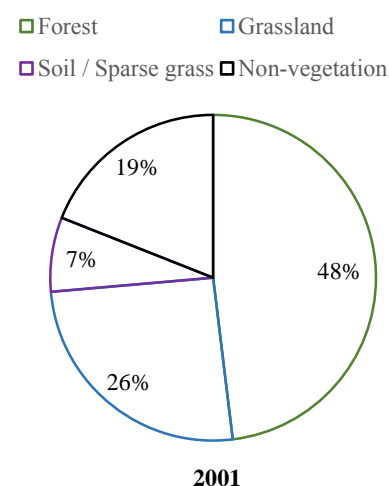
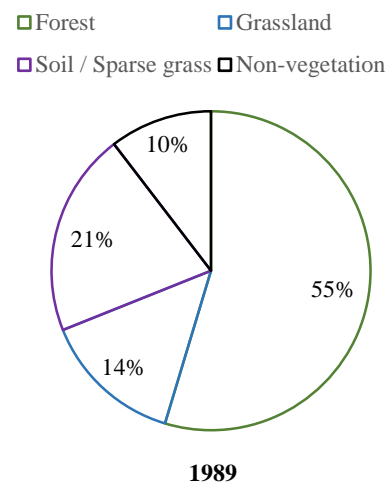


**Figure 4** The proportion of each land cover in 1989 and 2001

#### 3.2 Carbon loss

Caused by the deforestation and exploitation of soils, the total carbon potentials displayed a deceased trend. From 1989 to 2001 (Table 4), at least  $1.08 \times 10^8$  (Kg C) carbon potentials were depleted and the maximum losses would reach  $5.27 \times 10^8$  (Kg C). The median was  $2.83 \times 10^8$  (Kg C).

Comparing the result with previous study, Moraes et al (1998) also did a similar research in Rondonia, Brazil using a Landsat

		Initial 1989					
Final 2001	Area/ km <sup>2</sup>	Forest	Grassland	SSG	NVF	Row Total	Class Total
	<b>Forest</b>	146.66	24.14	9.08	0.87	180.75	180.75
	<b>Grassland</b>	30.97	16.98	33.24	14.84	96.03	96.03
	<b>SSG</b>	11.10	3.06	9.86	3.72	27.74	27.74
	<b>NVF</b>	16.76	9.50	25.48	19.68	71.42	71.42
	<b>Class Total</b>	205.50	53.69	77.66	39.11	0	0
	<b>Image Difference</b>	-24.75	42.34	-49.92	32.32	0	0

**Table 4** Change detection statistics

TM image that was acquired in 1991. They once suggested that during forest burning and decay of unburnt biomass release a considerable amount of carbon to atmosphere. In the research, the mosaic pastures that were converted from deforested land were discriminated of different ages. The results showed that the highest release of CO<sub>2</sub> to the atmosphere was  $1.104 \times 10^{12}$  Kg and occurred in the first three years after forest burning. The total amount of carbon released after twenty years was  $1.472 \times 10^{12}$  Kg. The comparison is illustrated in Table 5. By comparison, it can be concluded that forest shrink was the main cause of carbon losses (over half of total losses) around Rondonia.

	Comparison between 1989 and 2001	Moraes et al (1998)
<b>Study areas (km<sup>2</sup>)</b>	375	9200
<b>Carbon losses</b>	The highest loss in 12 years was $5.270 \times 10^8$ Kg C; Forest carbon loss was $2.97 \times 10^8$ Kg C	The total release of 20 years was $1.472 \times 10^{12}$ Kg; The highest release of $1.104 \times 10^{12}$ Kg; Forest biomass burning of $6.716 \times 10^{11}$ Kg

**Table 5** Comparing with the study of Moraes et al (1998)

### 3.3 The impact of carbon loss and deforestation

Through analysis, it could be inferred that carbon loss in NVR was mainly caused by deforestation and soil degradation. Such changes may result in effects on climate change, biological diversity, and other environmental influences (LU, 2006). In terms of carbon cycling process, the losses of carbon, which originally stored in vegetation, soils and other organic matters, were mainly discharged in forms of carbon dioxide (CO<sub>2</sub>). Basically, atmospheric CO<sub>2</sub> would be absorbed by photosynthesis, however, due to the deforestation and soil degradation, large amount of CO<sub>2</sub> could not be absorbed which resulted in the increase of CO<sub>2</sub> concentration.

The increase of CO<sub>2</sub> would lead to the climate change. According to Cao and Woodward (1998), who used terrestrial biogeochemical model to quantify the dynamic variations in ecosystem carbon fluxes from 1861 to 2070 in northern,

temperate and tropical areas. They estimated that between the 1860s and the 2060s, CO<sub>2</sub> increases from 288 to 640 p.p.m.v., and global terrestrial temperature rises from 12.5 to 15.5 °C.

### 3.4 The impact of carbon loss and deforestation

It has been found that traditional optical sensors still have insufficiencies in practical use. On the one hand, they are vulnerable to climate and atmospheric conditions that they are hardly to capture the textures and even spectral signals of LCs in cloudy or rainy days. On the other hand, they are not able to construct the structure of LCs, even if some studies simulated the structures by means of index models, such as NDVI, RVI, LAI and etc.(Wulder, 1998, Guillevic et al., 2002, Lu and Shuttleworth, 2002), but still shows defects in physical and direct understanding. That would affect the LCs recognition and discrimination and thereby the estimation of carbon changes.

With the booming of non-optical sensors in recent years, increasing of studies have been exploring the methods of combinations of multi-source sensors in order to alleviate the external influences and resolve the problem of class homogeneity of LC discrimination. Researchers found that the estimation of biomass and other forest structures were got significantly improved by using the synergy of information obtained from multi-source sensors. There are couples of sensors have been discussing most these years. Lidar and Radar show the advantage on supplying the accurate height and biomass measurements in successional forest (Sang et al, 2007, Ban, 2003, Lim, 2003). Because radar backscatter in the P and L bands is highly correlated with major forest parameters and SAR L-band data have proven to be particularly valuable for AGB estimation (Sun et al. 2002). For example, Sang et al (2007) integrated the series of ERS-1 data and SPOT XS image and got a slight improved overall accuracy in discriminating different vegetation types. In this case, future study would pay more attention on experimenting effective combinations of sensors to improve the estimation accuracies.

## 4. CONCLUSION

In conclude, the study deems that the deforestation and soil degradation are the main causes of potential carbon losses in tropical areas. The carbon potentials decreased at least  $1.08 \times 10^8$  (Kg C) and reach maximum of  $5.27 \times 10^8$  (Kg C) in a span of 12 years. Climate, wildlife habitats and biodiversity would all be affected. The carbon losses are estimated by using changed areas

with published carbon potential data. In order to detect changed area, supervised classification was carried out and the training samples were selected based on the PCA and spectral signatures of LC. The used methods are still required to be improved on reducing the uncertainty and errors. In future, more attentions would be paid on studying effective combinations of sensors to improve the estimation accuracies.

## REFERENCES

Ban, Y. 2003, 'Synergy of multitemporal ERS-1 SAR and Landsat TM data for classification of agricultural crops', *Can. J. Remote Sensing*, Vol. 29, No. 4, pp. 518–526.

Bastos, T.X., Diniz, T.D. de A.S. 1982, 'Avaliacão do clima do Estado de Rondônia para o desenvolvimento agrícola', Boletim de Pesquisa No. 44, Empresa Brasileira de Pesquisa Agropecuária/Centro de Pesquisas Agropecuárias do Triângulo Mídi (EMBRAPA/CPATU), Belo Horizonte, Minas Gerais, Brazil, pp. 28.

Braswell, B. H., Hagen, S. C., Frolking, S. E., Salas, W. A. 2003, 'A multivariable approach for mapping sub-pixel land cover distributions using MISR and MODIS: Application in the Brazilian Amazon region', *Remote Sensing of Environment*, Vol. 87, pp. 243–256.

Foody, G. M., Boyd, D. S., Cutler, M.E.J. 2003, 'Predictive relations of tropical forest biomass from Landsat TM data and their transferability between regions', *Remote Sensing of Environment*, Vol. 85, pp. 463–474.

Gong, P., Howarth, P. J. 1992, 'Frequency-based contextual classification and gray-level vector reduction for land-use identification', *Photogrammetry Engineering & Remote Sensing*, Vol. 58, pp. 423–437.

Graca, P. M. L. D. A., Fearnside, M. P., Cerri, C. C. 1999, 'Burning of Amazonian forest in Acre, Rondônia, Brazil: biomass, charcoal formation and burning efficiency', *Forest Ecology and Management*, Vol. 120, pp. 179–19.

Guillevic, P., Koster, R.D., Surez, M.J., Bounoua, L., Collatz, G.J., Los, S.O., Mahanama, S.P.P. 2002, 'Influence of the interannual variability of vegetation on the surface energy balance—a global sensitivity study', *Journal of Hydrometeorology*, Vol. 3, 617–629.

Halme, M. and Tomppo, E., 2001, 'Improving the accuracy of multisource forest inventory estimates by reducing plot location error – a multicriteria approach', *Remote Sensing of Environment*, Vol. 78, pp. 321–327.

Li, C., Dai, Y., Zhao, J., Yin, J., Dong, J., 2014, 'Volcanic ash cloud detection from remote sensing images using principal component analysis', *Computers and Electrical Engineering*, Vol. 40, pp. 204–214.

Lim, K., Treitz, P., Wulder, M., St-Onge, B., Flood, M., 2003, 'Lidar remote sensing of forest structure', *Progress in Physical Geography*, Vol. 27, pp. 88–106.

Lin C. F., Peng, B. H., Wang, W. F., Kong, X. J. 2012, 'Research on PCA and KPCA self-fusion based MSTAR SAR automatic target recognition algorithm', *J Electron Sci Technol*, Vol. 10, No. 4, pp. 352–357.

Liu, H.X., Yi, Y.J., Yue, Y.S., Cui, B.S., 2020, 'Reducing the likelihood of carbon loss from wetlands by improving the spatial connections between high carbon patches' *Journal of Cleaner Production*, Vol. 267.

LU, D., 2006, 'The potential and challenge of remote sensing-based biomass estimation', *International Journal of Remote Sensing*, Vol. 27, No. 7, pp. 1297–1328.

Lu, L.X., Shuttleworth, W.J. 2002, 'Incorporating NDVI-derived LAI into the climate version of RAMS and its impact on regional climate', *Journal of Hydrometeorology*, Vol. 3, pp. 347–362.

Moraes, J.F.L., Seyler, F., Cerri, C.C., Volkoff, B. 1998, 'Land cover mapping and carbon pools estimates in Rondonia, Brazil', *Remote Sensing*, Vol. 19, No. 5, pp. 921–934.

Myers, N. 1991, 'Tropical forests: present status and future outlook.' *Climatic Change*, Vol. 19, pp. 3–32.

Olson, J.S., Watts, J.A., Allison, L.J. 1983, 'Carbon in Live Vegetation of Major World Ecosystems', pp. 50–51. Oak Ridge: Oak Ridge National Laboratory. 180 pp.

Pirez, J. M., and Prance, G. T., 1986, 'The vegetation types of the Brazilian Amazon', in Prance, G. T. and Lovejoy, T. M. (eds) *Amazonia*, Pergamon Press, Oxford, pp. 109–115.

Sang, H., Lin, H., Yang, L., Liu, Y., Xiao, X. 2007, 'Land Cover Classification in the Poyang Lake Region, China, Using Landsat TM and JERS-1 Synthetic Aperture Radar Data', *Geographic Information Sciences*, Vol. 13:1–2, pp. 36–43.

Spanner, M., Johnson, L., Miller, J., McCreight, R., Freemantle, J., Runyon, J. and Gong, P. 1994, 'Remote sensing of seasonal leaf area index across the Oregon transect', *Ecological Applications*, Vol. 4, pp. 258–271.

Steininger, M. K. 2000, 'Satellite estimation of tropical secondary forest aboveground biomass data from Brazil and Bolivia.' *International Journal of Remote Sensing*, Vol. 21, pp. 1139–1157.

Sun, G., Ranson, K.J., Kharuk, V.I., 2002, 'Radiometric slope correction for forest biomass estimation from SAR data in the western Sayan Mountains, Siberia', *Remote Sensing of Environment*, Vol. 79, pp. 279–287.

Wulder, M., 1998, 'Optical remote-sensing techniques for the assessment of forest inventory and biophysical parameters', *Progress in Physical Geography*, Vol. 22, No. 4, pp. 449–476.

Zheng, D., Rademacher, J., Chen, J., Crow, T., Bressee, M., Le Moine, J., Ryu, S. 2004, 'Estimating aboveground biomass using Landsat 7 ETM+ data across a Biomass estimation managed landscape in northern Wisconsin, USA.', *Remote Sensing of Environment*, Vol. 93, pp. 402–411.

Zhao, Q., Xie, Z.L., Li, H., Li, X.L. 2012, 'Color-feature extraction of remote sensing image based on principal components analysis and K-means', *Microelectronic Computer*, Vol. 29, No. 10, pp. 61–68.

Zitova, B., Flusser, J. 2003, 'Image registration methods: a survey', *Image and Vision Computing*, Vol. 21, pp. 977-1000.